# Accepted Manuscript


A novel photoelectrochemical immunosensor for protein kinase activity assay based on phosphorylated graphite-like carbon nitride

Xue Li, Yunlei Zhou, Yan Xu, Huijie Xu, Minghui Wang, Huanshun Yin, Shiyun Ai

PII: S0003-2670(16)30787-5

DOI: 10.1016/j.aca.2016.06.024

Reference: ACA 234648

To appear in: *Analytica Chimica Acta*

Received Date: 8 April 2016

Revised Date: 9 June 2016

Accepted Date: 16 June 2016

Please cite this article as: X. Li, Y. Zhou, Y. Xu, H. Xu, M. Wang, H. Yin, S. Ai, A novel photoelectrochemical immunosensor for protein kinase activity assay based on phosphorylated graphite-like carbon nitride, *Analytica Chimica Acta* (2016), doi: 10.1016/j.aca.2016.06.024.

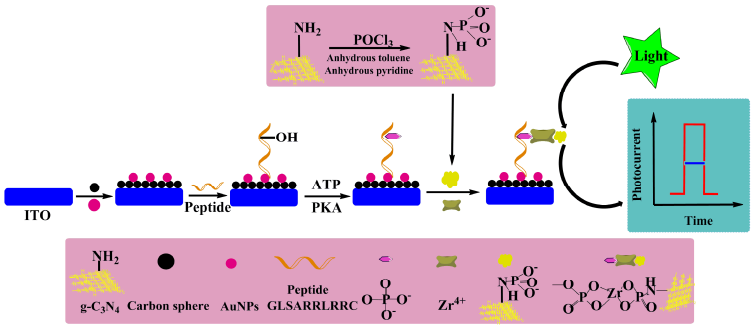

# A novel photoelectrochemical immunosensor for protein kinase activity assay based on phosphorylated graphite-like carbon nitride

Xue Li, Yunlei Zhou, Yan Xu, Huijie Xu, Minghui Wang, Huanshun Yin*, Shiyun Ai *

*College of Chemistry and Material Science, Shandong Agricultural University, Taian, 271018, P. R. China.*

* Corresponding authors:

Tel: +86 538 8249248

Fax: +86 538 8242251

*E-mail address*: yinhs@sdau.edu.cn (Huanshun Yin), ashy@sdau.edu.cn (Shiyun Ai).

**Abstract:** Protein kinases are general and significant regulators in the cell signaling pathway, and it is still greatly desired to achieve simple and quick kinase detection. Herein, we develop a simple and sensitive photoelectrochemical strategy for the detection of protein kinase activity based on the bond between phosphorylated peptide and phosphorylated graphite-like carbon nitride (P-g-$C_3N_4$) conjugates triggered by $Zr^{4+}$ ion coordination. Under optimal conditions, the increased photocurrent is proportional to the protein kinase A (PKA) concentration ranging from 0.05 to 50 U/mL with a detection limit of 0.077 U/mL. Moreover, this photoelectrochemical assay can be also applied to quantitative analysis of kinase inhibition. The results indicated that the $IC_{50}$ value (inhibitor concentration producing 50% inhibitor) for ellagic acid was 9.1 μM. Moreover, the developed method is further applied to detect PKA activity in real samples, which contains serum from healthy person and gastric cancer patients and breast tissue from healthy person and breast cancer patients. Therefore, the established protocol provides a new and simple tool for assay of kinase activity and its inhibitors with low cost and high sensitivity.

**Keywords:** Photoelectrochemical biosensor; Protein kinase activity; Phosphorylated graphite-like carbon nitride; Inhibitor; Real samples

## 1. Introduction

Photoelectrochemical (PEC) biosensor is a kind of novel and promising detection approach for biological assay with high sensitivity, low background current and simple instrument owing to the separation of electrochemical detection signals and the excitation source [1-3], which has aroused great concern in many aspects such as the detection of enzyme [4], DNA damage[5], subgroup J of avian leukosis virus [1] and small molecule [6]. Thus, we consider that PEC biosensor might be a desired platform for detecting protein kinase activity. As we all know, photoactive material is one of the dominant factors for the performance of PEC biosensor. Photoactive materials utilized in the PEC analysis include ZnS, $TiO_2$, ZnO and $Bi_2S_3$ and so on. For instance, Li et al. reported molecularly imprinted polymer modified $TiO_2$ nanotube arrays for PEC sensing of perfluorooctane sulfonate [7]. Tu et al. constructed a PEC biosensor of free-base-functionalized ZnO nanoparticles [8]. Sun et al. developed a PEC strategy for subgroup J avian leukosis virus immunoassay based on $Bi_2S_3$ nanorods [1]. However, it is well known that the wide bandgap (3.2 eV) of $TiO_2$ impedes intrinsic PEC response under visible light [9], and ZnO suffers from its instability. Also, they are metal-contained, which do not match well with a friendly environment. In consideration of those, it is necessary to develop new photoactive material with environment friendly property.

Recently, as a metal-free semiconductor and the most stable allotrope of carbon nitride material, graphite-like carbon nitride (g-$C_3N_4$) has become a hot topic. The appealing tri-*s*-triazine ring structure and the medium-gap (2.7 eV) of g-$C_3N_4$ make it

own high stability and an excellent photocatalytic activity with visible light irradiation ($\lambda$ < 460 nm). Due to its high stability, visible light response and unique electronic band structure, g-$C_3N_4$ has attracted increasing attention g-$C_3N_4$ and has been successfully widely applied in many fields, such as photocatalytic water splitting, sensing, photocatalysis and electrocatalysis [10-12]. Recent researches have demonstrated the promising application of g-$C_3N_4$ in PEC assay. For instance, Li et al. developed a novel multi-amplification PEC immunoassay for NMP-22 detection based on copper (II) enhanced polythiophene sensitized g-$C_3N_4$ nanosheet [3]. Bu et al. investigated the photo-to-current conversion properties and PEC cathodic protection performance of g-$C_3N_4$ in 304 stainless steel under visible or white light illumination [13]. Among these PEC assay, g-$C_3N_4$ and its compounds perform good PEC activity.

Protein phosphorylation catalyzed by protein kinases is a general and significant regulatory mechanism in the cell signaling pathways, which plays an important role in various crucial biological process in metabolism including cellular proliferation, apoptosis, differentiation and gene transcription [14, 15]. The over-expression and aberrant expression of protein kinases may lead to severe human diseases such as diabetes, cancer, cardiac diseases and inflammation [16]. Therefore, the simple, rapid and sensitive detection of protein kinase activity is a significant research for pathological process, clinical diagnosis and drug discovery. Traditionally, the detection method of protein kinase activity relied on radioactive adenosine triphosphate ($\gamma$-$^{32}$P-ATP) during the phosphorylation reaction [17], which is general

but harmful to the environment and human health. To overcome this defect, various kinase activity assays have been developed as the alternatives of radioactive assay, such as electrochemical [18, 19], surface-plasmon resonant [20], fluorophotometry [21] and mass spectroscopic techniques [22, 23] etc. In our work, PEC assay is chosen as desired detection method of protein kinase activity due to its high sensitivity, low background current and simple instrument. To achieve sensitive and simple detection, we fabricate a novel PEC method for protein kinase activity assay based on phosphorylated graphite-like carbon nitride (P-g-$C_3N_4$) nanoparticles as signal transduction probes, where P-g-$C_3N_4$ nanoparticles are obtained by simple chemical reaction based on amino of g-$C_3N_4$ according to the previous report with some proper modifications [24-26]. Because of its briefness, convenient and friendly environment advantages and no modification requirement for P-g-$C_3N_4$ and peptides, this developed strategy represents a potential application in protein kinase analysis.

## 2. Experimental

### *2.1 Reagents and instruments*

The substrate peptide (s-peptide, CRRLRRASLG) and adenosine 5'-triphosphate (ATP) disodium salt hydrate were obtained from Sangon Biotech Co., Ltd (Shanghai). Protein kinase A (PKA) catalytic subunit, mitogen-activated protein kinase (MAPK), casein kinase I (CK1) and casein kinase II (CK2) were supplied from New England Biolabs Ltd. (Beverly, MA). Radio immunoprecipitation assay (RIPA) lysis buffer and phenylmethanesulfonyl fluoride (PMSF) were purchased from Beyotime Biotech (Shanghai) Co., Ltd. Tris (hydroxymethyl) aminomethane

(Tris), gold chloride ($HAuCl_4$) and ascorbic acid (AA) were obtained from Aladdin (Shanghai, China). Zirconium oxychloride ($ZrOCl_2$) and phosphorus oxychloride ($POCl_3$) were purchased from Xiya Reagent Co., Ltd. (Chengdu, China). Indium Tin Oxide (ITO, coating 180 ± 25 nm, sheet resistance < 15 Ω/$cm^2$) slices were acquired from Zhuhai Kaivo Electronic Components Co., Ltd. (Zhuhai, China)). All other reagents are analytically purity graded and used without further purification.

The buffer solutions for this work is shown below. Peptide immobilization buffer, 20 mM Tris-HCl, 2.0 mM EDTA, 2.0 mM NaCl, 2.0 mM TCEP (pH = 7.4). PKA reaction buffer, 0.1 mM EDTA, 80 mM ATP, 2 mM DTT, 50 mM Tris-HCl, 10 mM $MgCl_2$, 0.01% Brij 35 (pH = 7.5). PKA storage buffer, 1 mM $Na_2EDTA$, 50 mM NaCl, 20 mM Tris-HCl, 2 mM DTT and 50% glycerol. Washing buffer (pH = 7.5), 10 mM Tris-HCl. Detection buffer, 100 mM PBS containing 100 mM AA. All reagents were of analytical purity. All of the aqueous solutions were prepared using redistilled deionized water, which was autoclaved.

Transmission electron microscope (TEM) images were taken with a JEOL-1200EX instrument (Japan). Fourier transformed infrared spectroscopy (FTIR) was obtained as KBr discs on a Nicolet 380 spectrometer. The photocurrent was recorded on a CHI832A electrochemical workstation (CHI instruments, Austin, USA) PEC measurements were carried out with a home-built PEC system with an additional three-electrode system. A modified ITO electrode (0.195 $cm^2$) was used as the working electrode. A saturated calomel electrode (SCE) and a Pt wire were applied as the reference electrode and the counter electrode. A 500 W Xe lamp equipped with

optical filter was employed as the irradiation source to produce the visible light, whose light intensity is 20 mW/cm$^2$. Electrochemical impedance spectroscopy (EIS) was performed on a CHI660C electrochemical workstation (CHI instruments, Austin, USA).

*2.2. Synthesis of carbon microspheres*

Carbon microspheres (CS) were prepared according to previous reports [27, 28]. Generally, glucose (3.2 g) was first dissolved into deionized water (70 mL) and mixed into a homogeneous solution under vigorous stirring. Then, the mixture was transferred into a Teflon-lined stainless steel antoclave of 100 mL capacity and maintained at 180 ºC for 3.5 h. After cooled to room temperature naturally, a dark precipitate was collected by centrifugation and washed successively with ethanol and deionized water several times. Finally, the obtained sample was dried under vacuum at 60 ºC.

*2.3 Synthesis of gold nanoparticles (AuNPs)*

AuNPs were prepared according to the previously reported method [29] with proper modifications. Typically, in a 100 mL two-necked flask, 5 mL of sodium citrate solution (38.8 mM) was rapidly added into 50 mL boiled $HAuCl_4$ solution (1 mM) under magnetic stirring. After a minute of stirring，the liquor's color was observed to change from light yellow to dark red. And then the mixture was maintained further boiling for 20 min. Finally, the obtained gold nanoparticles solution was stored at 4 ºC.

*2.4. Preparation of g-$C_3N_4$ and P-g-$C_3N_4$ nanoparticles*

g-$C_3N_4$ was synthesized according to previous report with some minor modifications [30]. In brief, an appropriate amount of dicyandiamide (DCDA) powder was put into an alumina crucible and heated in a tube furnace with a cover under ambient pressure in air. The alumina crucible containing DCDA powder was heated to different degrees and kept for different periods (The tube furnace with precursor is heated to 220 ℃ at a heating rate of 3 $K \cdot min^{-1}$ and maintained at 220 ℃ for 2 h, and then it is further heated to 350 ℃ and 550 ℃ and kept at these temperatures for 2 and 4 h, respectively). After completing the reaction, the products were cooled to 60 ℃ at a cooling rate of 3 $K \cdot min^{-1}$. Then rinsed by deionized water to remove soluble reactants and impurities, and ethanol to remove some organic impurities for several times. Since then, 20 mg g-$C_3N_4$ powder was dispersed in 6 mL double-distilled water at room temperature and exfoliated by ultrasonic process for 6 h. The final product was centrifuged and dried in vacuum at 60 ℃.

P-g-$C_3N_4$ nanoparticles were prepared according to the previous report with some minor modifications [24-26]. In brief, 44.6 mg of g-$C_3N_4$ was dispersed in 0.25 mL of anhydrous pyridine, and then 7.5 mL of anhydrous toluene solution and 0.25 mL of $POCl_3$ were added and the compound was incubated for 18 h at room temperature to obtain P-g-$C_3N_4$. Subsequently, the production was washed with toluene and deionized water, respectively. Finally, the resultant products were dried at 60 ℃ under vacuum.

*2.5 Biosensor fabrication*

The ITO conductive glasses were used as the working electrode, which were

cleaned by acetone, NaOH solution (1 M, in ethanol and distilled water with v/v = 1:1) and distilled water with sonication for 15 min, followed by washing thoroughly with distilled water and then dried at room temperature naturally before it was used.

2 mg of CS dark powder was weighed accurately and dispersed ultrasonically in 1 mL of double distilled deionized water, and then 20 μL of the suspension was dropped onto a piece of ITO electrode. After being dried in air, the CS/ITO was rinsed with double distilled deionized water for three times. Then, 20 μL of AuNPs solution was further dropped on the electrode surface and dried under Xe lamp , followed by rinsing with double distilled deionized water for three times (The electrode was named as AuNPs/CS/ITO). Subsequently, the AuNPs/CS/ITO was incubated with 20 μL of peptide (1 μM, dissolved in 20 mM Tris-HCl containing 2.0 mM EDTA, 2.0 mM NaCl, 2.0 mM TCEP, pH 7.4) for 12 h in a humid chamber at ambient temperature. After rinsed with washing buffer to remove the un-immobilized peptide for three times, the obtained electrode was noted as Peptide/AuNPs/CS/ITO.

PKA-catalyzed phosphorylation was carried out according to the manufacturer's protocol. Briefly, 30 μL PKA reaction solution containing different concentrations of PKA was dropped on Peptide/AuNPs/CS/ITO surface and incubated for 40 min at 37 °C in a humid chamber. After that, the electrode was rinsed thoroughly with washing buffer (The obtained electrode is noted as P-Peptide/AuNPs/CS/ITO). Then, 40 μL of $Zr^{4+}$ reaction buffer containing 0.25 M $Zr^{4+}$ and 30% acetonitrile (in 1 mL water) was dropped on P-Peptide/AuNPs/CS/ITO surface and incubated for 12 h in a humid chamber. The obtained $Zr^{4+}$/P-Peptide/AuNPs/CS/ITO electrode was rinsed

with washing buffer for three times. Afterwards, 40 μL of P-g-$C_3N_4$ dispersion was dropped onto the above electrode for 12 h in a humid chamber at ambient temperature. The obtained electrode (named as P-g-$C_3N_4$/$Zr^{4+}$/P-Peptide/AuNPs/CS/ITO) was rinsed for three times with washing buffer for the following measure.

For inhibiting the activity of PKA, different concentrations of ellagic acid were introduced into the PKA reaction solution and incubated for 40 min at 37 ℃. Then the electrode was rinsed copiously with the washing buffer and treated with $Zr^{4+}$ and P-g-$C_3N_4$ successively as described above.

*2.6 Detection of PKA activity in real samples*

Phosphorylation reaction was achieved by incubation of the S-peptide with gastric cancer serum sample and breast cancer tissue for 40 min at 37 ℃ and normal serum sample and breast tissues were used as control. Total protein extraction process was as follows. Breast cancer tissue was dealed with normal Saline for three times. The tissue was grinded for three times in RIPA lysis buffer containing PMSF solution (1 mM), DNA reaction buffer (100 mM), EDTA (50 mM) and DNase (0.25 U/μL) with the assistance of the liquid nitrogen. The homogenates were centrifuged at 12000 rpm for 20 min at 4 ℃. Then, the obtained supernatants were determined by UV-vis spectrophotometry. Also, cell lysates were diluted to 1 mg/mL total protein concentration for kinase activity assay.

**3. Result and discussion**

*3.1 Dectection strategy*

Scheme 1

In this work, a novel PEC method was developed for assay of protein kinase A activity using P-g-$C_3N_4$ as signal transduction probes. As seen in Scheme 1, the cysteine-terminated kemptides (CRRLRRASLG) were firstly assembled on the AuNPs/CS/ITO electrode surface through the Au-S bond between AuNPs and –SH to form a dense assemble layer. Then the serine residue containing the sequence of "LRRAS" can be phosphorylated by PKA, which can catalyze the transfer of γ-phosphoryl from ATP to the hydroxyl group of serine in the presence of ATP. Subsequently, $Zr^{4+}$ is selected as the identifying reagent for the phosphate group. The high affinity between $Zr^{4+}$ and the phosphate group causes the assembly of P-g-$C_3N_4$ on the substrate peptide. Finally, as electron donor, AA can provide one electron for capturing the photo-generated hole and decreasing the recombination probability of photo-generated electron and hole of the immobilized P-g-$C_3N_4$, which results in an increased photocurrent. Through the relationship between the photocurrent and PKA concentration, the PKA can be detected. This work mainly performs its advantages in two aspects. On one hand, the photoactive material of P-g-$C_3N_4$ is "green" and hazardous-free to environment compared with other metal-contained materials. On the other hand, P-g-$C_3N_4$ can be excited by visible light, which can avoid the damage of UV-light to biomolecules.

*3.2 Characterization of CS, g-$C_3N_4$, P-g-$C_3N_4$ and different electrodes*

Fig. 1.

These regular spheres concentrate on 220~240 nm with a diameter of ca. 200 nm between them, which could be clearly seen from TEM image (Fig. 1A). The spheres

with homogeneous and regular morphology can be spread out on the electrode surface flatly. What's more, Fig. 1B shows the TEM image of the prepared pure g-$C_3N_4$ sample with the diameter about 100 nm, which reveals a clearly flat layer structure. To characterize the construction process of the modified electrode, different modification electrodes were characterized by EIS in 5 mM $K_3[Fe(CN)_6]/K_4[Fe(CN)_6]$ mixture containing 0.1 M KCl. As depicted in Fig. 1C, after the AuNPs or g-$C_3N_4$ nanoparticles were modified onto the bare ITO electrode with an Ret value about 190 Ω, the semicircle decreased (Fig. 1C, curve a and curve b), indicating that the immobilized AuNPs or g-$C_3N_4$ nanoparticles promoted the electron transfer process on the electrode surface. Compared with g-$C_3N_4$/ITO electrode (curve b), the Nyquist plot of P-g-$C_3N_4$/ITO electrode (curve d) shows a bigger semicircle with a $R_{et}$ value about 300 Ω. It can be attributed to the negative charge of P-g-$C_3N_4$, which hinders the electron transfer. The Ret value significantly increased with P-peptide, $Zr^{4+}$ and P-g-$C_3N_4$ immobilized onto the AuNPs/CS/ITO successively. It can be attributed to the hindrance effect, which hinders the electron transfer and increases the $R_{et}$ value. In addition, to testify the product of P-g-$C_3N_4$, the active material of P-g-$C_3N_4$ can be further verified by compared FTIR spectra of g-$C_3N_4$ with P-g-$C_3N_4$. From the Fig. 1D (a), there are some specific absorption peaks of g-$C_3N_4$. The peak located in 812 $cm^{-1}$ is attributed to aromatic structure vibration peak of g-$C_3N_4$ triazine ring, which are extremely typical specific absorption peaks of g-$C_3N_4$. Moreover, the absorption peaks from 1200 $cm^{-1}$ to 1650 $cm^{-1}$ indicate the existence of a large amount of C−N and C=N. What's more, the broad bands located at 3300~3500 $cm^{-1}$ are related to

stretching vibration of the amino. Similarly, some specific absorption peaks belong to P-g-$C_3N_4$ (Fig. 1D (b)). The absorption peaks at 880 $cm^{-1}$ (P-O), 1084 $cm^{-1}$ (P-N) 1244 $cm^{-1}$ (P=O) are found, which are consistent with the previous report [31]. Similarly, the absorption peaks from 1200 $cm^{-1}$ to 1650 $cm^{-1}$ indicate the existence of a large amount of C−N and C=N. Therefore, the above results indicate the completion of P-g-$C_3N_4$.

*3.3 Detection feasibility assay*

Fig. 2.

For demonstrating the detection feasibility of the developed biosensor for PKA activity assay, the photocurrents of different electrodes are recorded in 0.1 M PBS containing 0.1 M AA (pH 7.4). From the Fig. 2, the photocurrent of $Zr^{4+}$/P-peptide/AuNPs/CS/ITO (curve a) decreases when the substrate peptide is assembled on the AuNPs/CS/ITO electrode surface (curve c), which is consistent with the steric-hindrance effect of peptide. More importantly, as shown in Fig. 2, only a weak photocurrent is observed for $Zr^{4+}$/P-peptide/AuNPs/CS/ITO (curve a). After immobilization of P-g-$C_3N_4$, an enhanced photocurrent is observed (curve d), which is ascribed to the capture of P-g-$C_3N_4$ with the good photoelectric performance. What's more, in order to testify the significance of the phosphorylation event in the assay of PKA activity, the photocurrent of Peptide/AuNPs/CS/ITO was compared when it was treated with and without PKA. When peptide/AuNPs/CS/ITO electrode was incubated with $Zr^{4+}$ and P-g-$C_3N_4$ directly, almost no P-g-$C_3N_4$ is adsorbed on peptide/AuNPs/CS/ITO in the absence of PKA, which is observed with a lower

photocurrent of peptide/AuNPs/CS/ITO (curve b) than P-g-$C_3N_4$/$Zr^{4+}$/P-peptide/AuNPs/CS/ITO (curve d). The results indicate peptide can not be phosphorylated without incubated with PKA, which leads to the failure of capture of P-g-$C_3N_4$. Consequently, the phototcurrent is weak because of the absence of electron donor of AA in the detection buffer. Based on the above researches, we believe that the developed method can be applied to analysing PKA activity.

*3.4 Optimization of P-g-$C_3N_4$ concentration and PKA incubation time*

Fig. 3.

For PEC biosensor, the concentration of photoactive material is an important parameter, which influences the detection sensitivity. Thus the P-g-$C_3N_4$ concentration is optimized in detail. As seen in Fig. 3A, the photocurrent enhances with the increase in the P-g-$C_3N_4$ concentration from 0.5 to 2.0 mg/mL, which generates more photoelectron, resulting in an enhanced PEC response. When the P-g-$C_3N_4$ concentration exceeds 2.0 mg/mL, the photocurrent levels off. It can be explained as when the activity of PKA is constant, the P-peptide is fixed and then the $Zr^{4+}$ and P-g-$C_3N_4$ are fixed. Thus, considering the detection efficiency, 2.0 mg/mL of P-g-$C_3N_4$ is used in the following experiments.

In the proposed system, the phosphorylation time is found to be crucial for the kinase-catalyzed reaction on the electrode surface. As presented in Fig. 3B, with increasing the phosphorylation time, the photocurrent increases quickly from 5 to 40 min, and then levels off when further prolonging the phosphorylation time. Thus, 40 min is chosen as the optimal phosphorylation time.

*3.5 PKA activity assay*

Fig. 4.

Under optimum conditions, PKA activity is evaluated with different concentrations of PKA. When the PKA concentration increases from 0.05 to 50 U/mL, the photocurrent enhances accordingly (Fig. 4A) and reaches a saturation value once the concentration of PKA is above 50 U $mL^{-1}$. The dependence of the photocurrent response on the PKA concentration is presented in Fig. 4B. There is a good linear relationship in the range of 0.05 to 50 U/mL with linear regression equation of $I$ (nA) =88.76log$c$ (U/mL) + 233.9 ($R$ = 0.9947), and the detection limit is calculated to be 0.077 U/mL. In regard to detection sensitivity, the developed PKA activity detection method was better than most of reported works, as listed in Table 1, which indicated that the PEC biosensor in this work might be a desired detection platform for protein kinase activity assay. As a potentially applicable immunoassay, the specificity and reproducibility of the biosensor are essential criterions. Therefore, for investigating the specificity, the peptide/AuNPs/CS/ITO electrode is first incubated with 50 U/mL of PKA, CK1, CK2 and MAPK, respectively. Subsequently, the obtained electrode is further incubated with $Zr^{4+}$ and P-g-$C_3N_4$. Finally, the photocurrent responses are recorded in 0.1 M PBS containing 0.1 M AA (pH 7.4.). As depicted in Fig. 4C, the photocurrent change ($\Delta I = I_1$-$I_2$) is compared, where $I_1$ is the photocurrent of peptide/AuNPs/CS/ITO electrode incubated with kinase, $Zr^{4+}$ and P-g-$C_3N_4$ successively, $I_2$ is the photocurrent of peptide/AuNPs/CS/ITO electrodes. The result reveals that the $\Delta I$ of the peptide/AuNPs/CS/ITO electrodes incubated with CK1, CK2

and MAPK are much lower than that obtained for PKA, indicating that it had acceptable detection specificity. In addition, as shown in Fig. 4D, the fabricated PEC biosensor for PKA activity detection showed good reproducibility and the relative standard deviation is 1.34% evaluated by performing the photocurrent responses of ten repeatedly prepared P-g-$C_3N_4$/$Zr^{4+}$/P-peptide/AuNPs/CS/ITO electrodes.

*3.6 Inhibition assay*

Fig. 5.

The screening of kinase inhibitor is extremely important based on its potential for disease therapy. In the inhibition assay, the P-$C_3N_4$ mediated PEC biosensor was also used to quantitatively evaluate the inhibition of kinase by mixing PKA and varying concentrations of ellagic acid (a well-recognized effient inhibitor of PKA). As seen from Fig. 5, with increasing concentration of ellagic acid, the activity inhibition percent increases gradually, indicating a low activity of PKA and peptide phosphorylation level. The maximal activity inhibition percent is observed with the addition of ellagic acid at 12 μM. On the basis of the results, it proves the inhibition effects of ellagic acid on PKA activity, and the $IC_{50}$ value (the half-maximal inhibitory concentration) of ellagic acid is measured to be 9.1 μM, which is a little higher than some of previous reports, such as 5.33 and 3.7 μM [41, 42], indicating that the developed biosensor might be need to further improved for inhibitor screening.

*3.7 Detection of PKA activity in real samples*

Fig. 6.

To test the applicability of the developed PEC sensor for PKA activity detection

in real samples, PKA activity in human serum of gastric cancer and human breast cancer tissue is detected by the above sensor. As control, the PKA activity in normal samples is also detected. As can be seen from Fig. 6, the relative expression of PKA activity in gastric cancer serum exhibits significant enhancement when compared with control results, indicating that PKA activity is improved in gastric cancer serum. To prove the accuracy of this method, the expression level of PKA activity in breast cancer tissue is also investigated (Fig. 6). The results indicate that PKA activity is increased in breast cancer cell sample similarly. These evaluations suggest a great potential of the developed sensor for the monitoring of PKA activity in different cancer samples for early diagnosis of cancers.

## 4. Conclusion

In conclusion, we develop a novel PEC method for protein kinase activity assay and inhibitor screening based on a kind of novel signal transduction probe of P-g-$C_3N_4$. This strategy provides a simple detection procedure owing to the cheap precursor and easy preparation for P-g-$C_3N_4$. Moreover, the photoactive material of P-g-$C_3N_4$ is metal-free, which completely avoids the risk of environmental pollution from metal element. As a result, the fabricated PEC biosensor performs a highly sensitive detection for PKA activity with a low detection limit of 0.077 U/mL. Furthermore, this proposed strategy is also successfully applied to inhibition screening and PKA activity detection in real samples, indicating great potential in the kinase-related clinic diagnostics and drug discovery applications.

## Acknowledgements

This work was supported by the National Natural Science Foundation of China (No. 21375079), the Natural Science Foundation of Shandong province, China (No. ZR2014BQ029), China Postdoctoral Science Foundation (No. 2014M550369，No. 2015M582120) and the Project of Development of Science and Technology of Shandong Province, China (No. 2013GZX20109).

**References**

[1] B. Sun, F. Qiao, L. Chen, Z. Zhao, H. Yin, S. Ai, Effective signal-on photoelectrochemical immunoassay of subgroup J avian leukosis virus based on $Bi_2S_3$ nanorods as photosensitizer and in situ generated ascorbic acid for electron donating, Biosens. Bioelectron. 54 (2014) 237-243.

[2] H. Yin, M. Wang, Y. Zhou, X. Zhang, B. Sun, G. Wang, et al., Photoelectrochemical biosensing platform for microRNA detection based on in situ producing electron donor from apoferritin-encapsulated ascorbic acid, Biosens. Bioelectron. 53 (2014) 175-181.

[3] R. Li, Y. Liu, X. Li, S. Zhang, D. Wu, Y. Zhang, et al., A novel multi-amplification photoelectrochemical immunoassay based on copper(II) enhanced polythiophene sensitized graphitic carbon nitride nanosheet, Biosens. Bioelectron. 62 (2014) 315-319.

[4] X. Zhang, S. Li, X. Jin, S. Zhang, A new photoelectrochemical aptasensor for the detection of thrombin based on functionalized graphene and CdSe nanoparticles multilayers, Chem. Commun. 47 (2011) 4929-4931.

[5] Y. Liu, S. Jia, L.-H. Guo, Development of microplate-based photoelectrochemical

DNA biosensor array for high throughput detection of DNA damage, Sens. Actuators, B 161 (2012) 334-340.

[6] J. Gong, X. Wang, X. Li, K. Wang, Highly sensitive visible light activated photoelectrochemical biosensing of organophosphate pesticide using biofunctional crossed bismuth oxyiodide flake arrays, Biosens. Bioelectron. 38 (2012) 43-49.

[7] J. Li, H. Feng, J. Cai, L. Yuan, N. Wang, Q. Cai, Molecularly imprinted polymer modified $TiO_2$ nanotube arrays for photoelectrochemical determination of perfluorooctane sulfonate (PFOS), Sens. Actuators, B 190 (2014) 745-751.

[8] W. Tu, J. Lei, P. Wang, H. Ju, Photoelectrochemistry of Free-Base-Porphyrin-Functionalized Zinc Oxide Nanoparticles and Their Applications in Biosensing, Chem.--Eur. J. 17 (2011) 9440-9447.

[9] T. Tachikawa, S. Yamashita, T. Majima, Evidence for Crystal-Face-Dependent $TiO_2$ Photocatalysis from Single-Molecule Imaging and Kinetic Analysis, J. Am. Chem. Soc. 133 (2011) 7197-7204.

[10] X. Wang, S. Blechert, M. Antonietti, Polymeric Graphitic Carbon Nitride for Heterogeneous Photocatalysis, ACS Catal. 2 (2012) 1596-1606.

[11] J. Tian, R. Ning, Q. Liu, A.M. Asiri, A.O. Al-Youbi, X. Sun, Three-Dimensional Porous Supramolecular Architecture from Ultrathin g-$C_3N_4$ Nanosheets and Reduced Graphene Oxide: Solution Self-Assembly Construction and Application as a Highly Efficient Metal-Free Electrocatalyst for Oxygen Reduction Reaction, ACS Appl. Mater. Interfaces 6 (2014) 1011-1017.

[12] H. Zhang, Q. Huang, Y. Huang, F. Li, W. Zhang, C. Wei, et al., Graphitic carbon

nitride nanosheets doped graphene oxide for electrochemical simultaneous determination of ascorbic acid, dopamine and uric acid, Electrochim. Acta 142 (2014) 125-131.

[13] Y. Bu, Z. Chen, J. Yu, W. Li, A novel application of g-C3N4 thin film in photoelectrochemical anticorrosion, Electrochim. Acta 88 (2013) 294-300.

[14] Z.-F. Zhang, H. Cui, C.-Z. Lai, L.-J. Liu, Gold Nanoparticle-Catalyzed Luminol Chemiluminescence and Its Analytical Applications, Anal. Chem. 77 (2005) 3324-3329.

[15] X. Zhou, D. Xing, D. Zhu, L. Jia, Magnetic Bead and Nanoparticle Based Electrochemiluminescence Amplification Assay for Direct and Sensitive Measuring of Telomerase Activity, Anal. Chem. 81 (2009) 255-261.

[16] H. Wang, A. Davis, S. Yu, K. Ahmed, Response of cancer cells to molecular interruption of the CK2 signal, in: K. Ahmed, O.-G. Issinger, J. Allende (Eds.), Protein Kinase CK2 — From Structure to Regulation, Springer US2001, pp. 167-174.

[17] B.T. Houseman, J.H. Huh, S.J. Kron, M. Mrksich, Peptide chips for the quantitative evaluation of protein kinase activity, Nat. Biotechnol. 20 (2002) 270-274.

[18] T. Yoshida, M. Sato, T. Ozawa, Y. Umezawa, An SPR-Based Screening Method for Agonist Selectivity for Insulin Signaling Pathways Based on the Binding of Phosphotyrosine to Its Specific Binding Protein, Anal. Chem. 72 (2000) 6-11.

[19] X. Xu, Z. Nie, J. Chen, Y. Fu, W. Li, Q. Shen, et al., A DNA-based electrochemical strategy for label-free monitoring the activity and inhibition of protein kinase, Chem. Commun. (2009) 6946-6948.

[20] Y. Yang, L.-H. Guo, N. Qu, M.-Y. Wei, L.-X. Zhao, B. Wan, Label-free electrochemical measurement of protein tyrosine kinase activity and inhibition based on electro-catalyzed tyrosine signaling, Biosens. Bioelectron. 28 (2011) 284-290.

[21] M.D. Allen, L.M. DiPilato, M. Rahdar, Y.R. Ren, C. Chong, J.O. Liu, et al., Reading Dynamic Kinase Activity in Living Cells for High-Throughput Screening, ACS Chem. Biol. 1 (2006) 371-376.

[22] J.D. Dunn, G.E. Reid, M.L. Bruening, Techniques for phosphopeptide enrichment prior to analysis by mass spectrometry, Mass Spectrom. Rev. 29 (2010) 29-54.

[23] M. Mann, S.-E. Ong, M. Grønborg, H. Steen, O.N. Jensen, A. Pandey, Analysis of protein phosphorylation using mass spectrometry: deciphering the phosphoproteome, Trends Biotechnol. 20 (2002) 261-268.

[24] W. Ren, C. Liu, S. Lian, Z. Li, Flow Cytometry-Assisted Mix-and-Read Assay for Ultrasensitive Detection of Protein Kinase Activity by use of $Zr^{4+}$-Functionalized Mesoporous $SiO_2$ Microspheres, Anal. Chem. 85 (2013) 10956-10961.

[25] L. Zhao, R.a. Wu, G. Han, H. Zhou, L. Ren, R. Tian, et al., The Highly Selective Capture of Phosphopeptides by Zirconium Phosphonate-Modified Magnetic Nanoparticles for Phosphoproteome Analysis, J. Am. Soc. Mass. Spectrom. 19 (2008) 1176-1186.

[26] L. Hu, H. Zhou, Y. Li, S. Sun, L. Guo, M. Ye, et al., Profiling of Endogenous Serum Phosphorylated Peptides by Titanium (IV) Immobilized Mesoporous Silica Particles Enrichment and MALDI-TOFMS Detection, Anal. Chem. 81 (2009) 94-104.

[27] Y. Mi, W. Hu, Y. Dan, Y. Liu, Synthesis of carbon micro-spheres by a glucose

hydrothermal method, Mater. Lett. 62 (2008) 1194-1196.

[28] M. Li, W. Li, S. Liu, Hydrothermal synthesis, characterization, and KOH activation of carbon spheres from glucose, Carbohydr. Res. 346 (2011) 999-1004.

[29] A. Cayuela, M.L. Soriano, M.C. Carrión, M. Valcárcel, Functionalized carbon dots as sensors for gold nanoparticles in spiked samples: Formation of nanohybrids, Anal. Chim. Acta. 820 (2014) 133-138.

[30] K.K. Han, C.C. Wang, Y.Y. Li, M.M. Wan, Y. Wang, J.H. Zhu, Facile template-free synthesis of porous g-C3N4 with high photocatalytic performance under visible light, RSC Adv. 3 (2013) 9465-9469.

[31] H. Ma, L. Tong, Z. Xu, Z. Fang, Y. Jin, F. Lu, A novel intumescent flame retardant: Synthesis and application in ABS copolymer, Polym. Degrad. Stab. 92 (2007) 720-726.

[32] J. Bai, Y. Zhao, Z. Wang, C. Liu, Y. Wang, Z. Li, Dual-readout fluorescent assay of protein kinase activity by use of $TiO_2$-coated magnetic microspheres, Anal. Chem. 85 (2013) 4813-4821.

[33] X. Xu, X. Liu, Z. Nie, Y. Pan, M. Guo, S. Yao, Label-free fluorescent detection of protein kinase activity based on the aggregation behavior of unmodified quantum dots, Anal. Chem. 83 (2010) 52-59.

[34] J. Zhou, X. Xu, W. Liu, X. Liu, Z. Nie, M. Qing, et al., Graphene oxide–peptide nanocomplex as a versatile fluorescence probe of protein kinase activity based on phosphorylation protection against carboxypeptidase digestion, Anal. Chem. 85 (2013) 5746-5754.

[35] P. Tan, C. Lei, X. Liu, M. Qing, Z. Nie, M. Guo, et al., Fluorescent detection of protein kinase based on zirconium ions-immobilized magnetic nanoparticles, Anal. Chim. Acta. 780 (2013) 89-94.

[36] S. Shiosaki, T. Nobori, T. Mori, R. Toita, Y. Nakamura, C.W. Kim, et al., A protein kinase assay based on FRET between quantum dots and fluorescently-labeled peptides, Chem. Commun. 49 (2013) 5592-5594.

[37] X. Xu, J. Zhou, X. Liu, Z. Nie, M. Qing, M. Guo, et al., Aptameric peptide for one-step detection of protein kinase, Anal. Chem. 84 (2012) 4746-4753.

[38] Y. Wang, L. Zhang, R.-P. Liang, J.-M. Bai, J.-D. Qiu, Using graphene quantum dots as photoluminescent probes for protein kinase sensing, Anal. Chem. 85 (2013) 9148-9155.

[39] Z. Chen, X. He, Y. Wang, K. Wang, Y. Du, G. Yan, Ru (II) encapsulated phosphorylate-terminated silica nanoparticles-based electrochemiluminescent strategy for label-free assay of protein kinase activity and inhibition, Biosens. Bioelectron. 41 (2013) 519-525.

[40] S. Xu, Y. Liu, T. Wang, J. Li, Highly sensitive electrogenerated chemiluminescence biosensor in profiling protein kinase activity and inhibition using gold nanoparticle as signal transduction probes, Anal. Chem. 82 (2010) 9566-9572.

[41] Z. Zhao, X. Zhou, D. Xing, Highly sensitive protein kinase activity assay based on electrochemiluminescence nanoprobes, Biosens. Bioelectron. 31 (2012) 299-304.

[42] J. Wang, M. Shen, Y. Cao, G. Li, Switchable "On-Off" electrochemical technique for detection of phosphorylation, Biosens. Bioelectron. 26 (2010) 638-642.

**Figure caption:**

**Scheme 1.** Schematic illustration of PEC strategy for kinase activity assay.

**Fig. 1.** (A) TEM images of CS. The inset graph is the size distribution of CS. (B) TEM images of g-$C_3N_4$. (C) EIS of AuNPs/CS/ITO (a), g-$C_3N_4$/ITO (b), ITO (c), P-g-$C_3N_4$/ITO (d), P-peptide/AuNPs/CS/ITO (e) and P-g-$C_3N_4$/$Zr^{4+}$/P-peptide/AuNPs/CS/ITO (f) in 5 mM $K_3[Fe(CN)_6]$/$K_4[Fe(CN)_6]$ mixture containing 0.1 M KCl. (D) FTIR spectra of g-$C_3N_4$ (a) and P-g-$C_3N_4$ (b). PKA concentration is 50 U/mL.

**Fig. 2.** The PEC response of different electrodes in 0.1 M PBS containing 0.1 M AA (pH 7.4.). a, $Zr^{4+}$/P-peptide/AuNPs/CS/ITO, b, peptide/AuNPs/CS/ITO was incubated with $Zr^{4+}$ and P-g-$C_3N_4$, c, AuNPs/CS/ITO, d, P-g-$C_3N_4$/$Zr^{4+}$/P-peptide/AuNPs/CS/ITO. PKA concentration is 50 U/mL.

**Fig. 3**. Effect of P-g-$C_3N_4$ concnetration (A) and PKA incubation time on the PEC response of the biosensor. PKA concentration is 50 U/mL.

**Fig. 4**. (A) The PEC response of the biosensor with different PKA concentrations. a-h: 0.05, 0.1, 0.5, 1, 5, 10, 30, 50 U/mL. (B) The linear correlation between PEC intensity and PKA concentrations. (C) The PEC response change of the biosensors with different protein kinase. The concentration of different protein kinase is 50 U/mL. (D)

The PEC response of ten biosensors fabricated independently. PKA concentration is 50 U/mL.

Fig. 5. The PEC response of the biosensor after inhibiting with different concentrations of ellagic acid. a-j: 0, 2, 4, 6, 8, 10, 12, 14, 16, 18 μM. Inset graph is the plot for the inhibition percent versus ellagic acid concentration. PKA concentration is 50 U/mL.

**Fig. 6**. The histogram of the relative activity of PKA in different samples..

Table 1. The comparison of the detection performance of the developed PEC assay with other methods for kinase activity

| Methods | Kinase | Linear range (unit/mL) | LOD (unit/mL) | Refs. |
|---|---|---|---|---|
| Fluorescence | PKA | 0.5-500 | 0.1 | [32] |
| Fluorescence | PKA | 0-400 | 0.47 | [33] |
| Fluorescence | PKA/CK2 | | 0.0833 | [34] |
| Fluorescence | PKA | 0-1000 | 0.5 | [35] |
| FRET | PKA | | 0.08 | [36] |
| Electrochemistry | PKA | | 0.15 | [19] |
| QCM | PKA | 0.64-22.33 | 0.061 | [37] |
| Photoluminescent | CK2 | 0.1–1 | 0.03 | [38] |
| ECL | PKA | 0.01-100 | 0.005 | [39] |
| ECL | PKA | 0.07-32 | 0.07 | [40] |
| ECL | PKA | 0-100 | 0.005 | [41] |
| PEC assay | PKA | 0.05–50 | 0.077 | This work |

ECL: electrochemiluminescence; QCM: quartz crystal microbalance; CK2: casein kinase 2; FRET: Fluorescence Resonance Energy Transfer

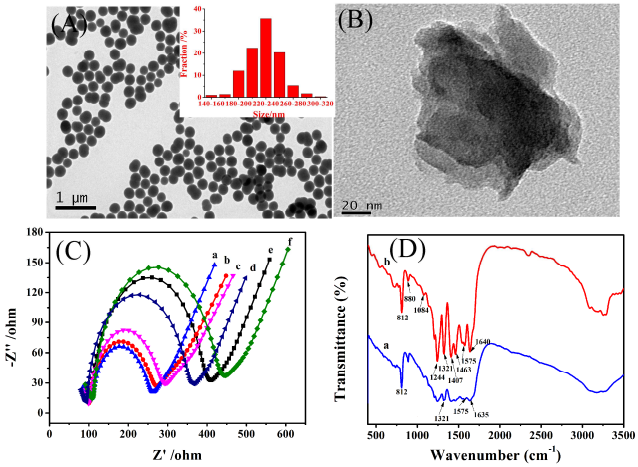

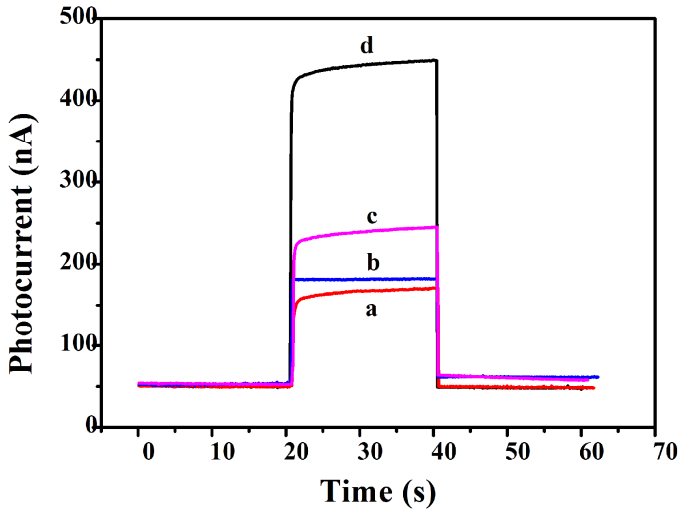

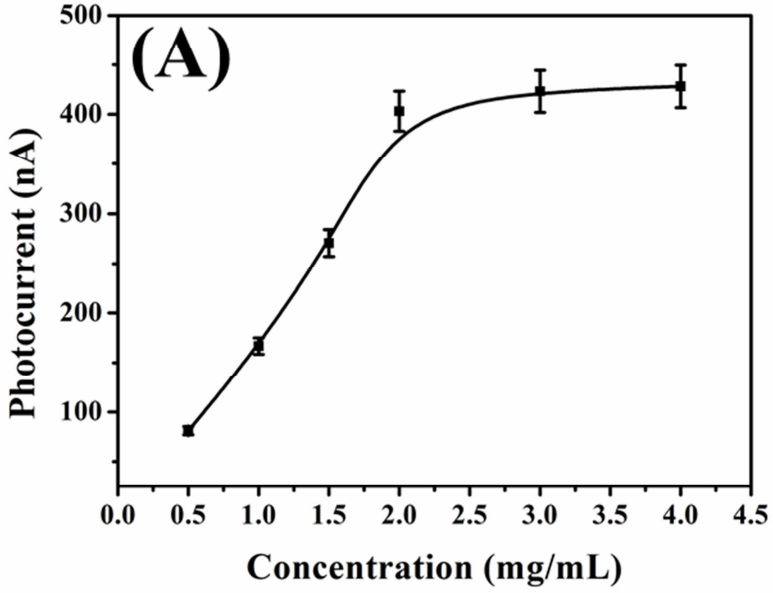
(A)
Photocurrent (nA)
500
400
300
200
100
0.0
0.5
1.0
1.5
2.0
2.5
3.0
3.5
4.0
4.5
Concentration (mg/mL)

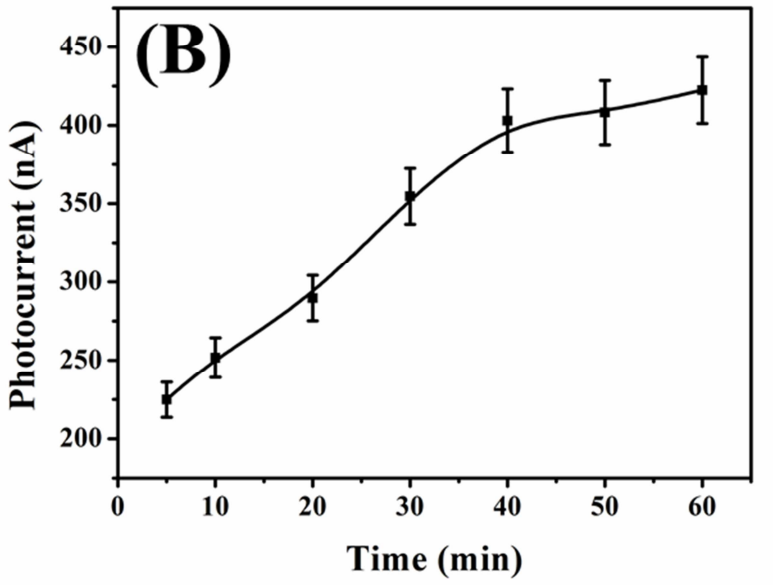
(B)
Photocurrent (nA)
450
400
350
300
250
200
0
10
20
30
40
50
60
Time (min)

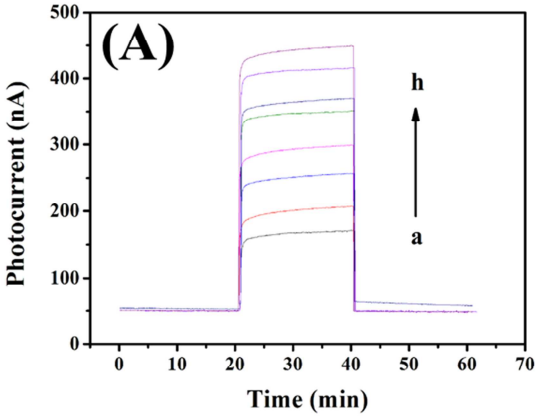
(A)
Photocurrent (nA)
Time (min)
h
a

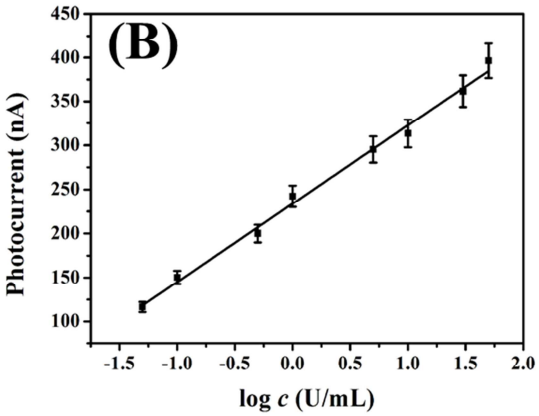
(B)
Photocurrent (nA)
log c (U/mL)

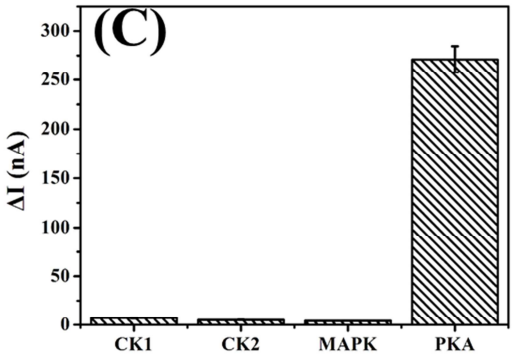
(C)
ΔI (nA)
CK1
CK2
MAPK
PKA

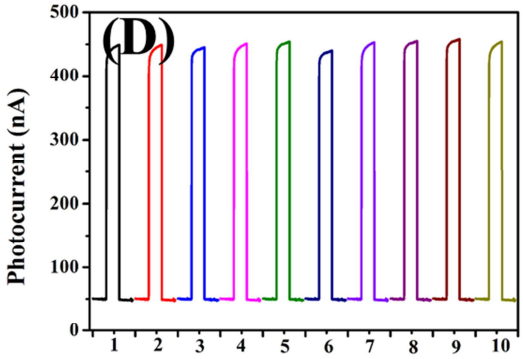
(D)
Photocurrent (nA)

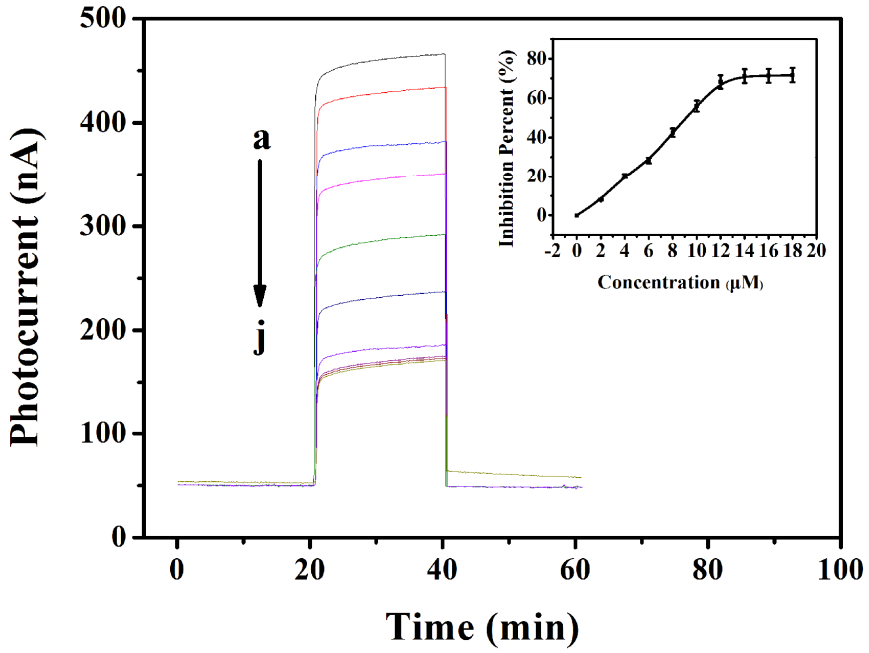

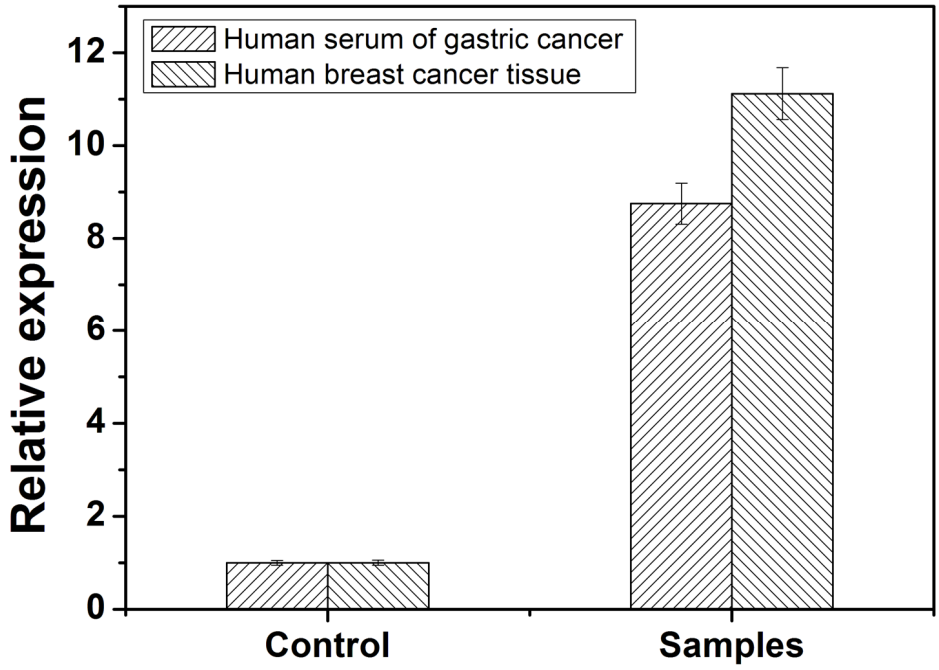

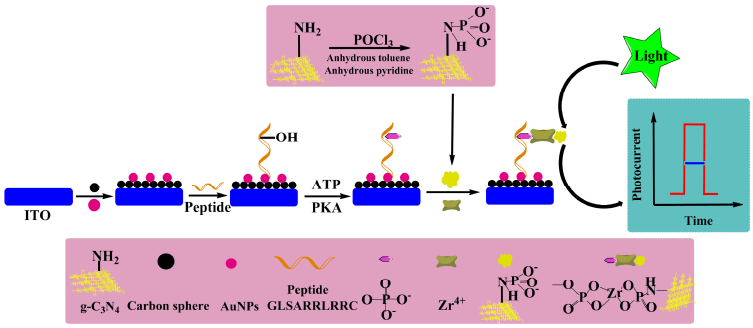

## Highlights

1. A novel photoelectrochemical biosensor is fabricated for kinase activity assay.

2. Phosphorylated g-$C_3N_4$ is used as the photoelectric conversion material with visible-light activity.

3. The high affinity between $Zr^{4+}$ and the phosphate group causes the assembly of P-g-$C_3N_4$ on the substrate peptide.

4. The developed method can be applied to detect kinase in real samples.